Inorganic Chemistry
Article

Inorg. Chem. **2010**, *49*, 969–976 **969**
DOI: 10.1021/ic901720a

Slow Relaxation Processes and Single-Ion Magnetic Behaviors in Dysprosium-Containing Complexes

Ying Wang, Xi-Li Li, Tian-Wei Wang, You Song,* and Xiao-Zeng You*

State Key Laboratory of Coordination Chemistry, Nanjing National Laboratory of Microstructures, School of Chemistry and Chemical Engineering, Nanjing University, Nanjing 210093, China

Received August 31, 2009

A series of one-dimensional complexes $[Ln(L_1)_3(HOCH_2CH_2OH)]_n$ (L_1 = 2-furoate anion; Ln = Nd (**1**), Sm (**2**), Gd (**3**), Tb (**4**), Dy (**5**), Er (**6**)) have been synthesized. The complexes were crystallized in the monoclinic space group *P*2(1)/*c* and show a chain-like structure determined by single-crystal X-ray diffraction. Magnetic properties indicate that carboxyl group of 2-furoate mediates different magnetic couplings in light and heavy rare earth complexes, namely, antiferromagnetic interaction between light rare earth ions and ferromagnetic interaction between heavy ones. Noticeably, complex **5** displays a strong frequency dependence of alternating current (AC) magnetic properties. Further magnetic studies show a distribution of a single relaxation process in **5**. While 1,10-phenanthroline and phthalate anion (L_2) were employed, $[Dy_2(L_2)_6(H_2O)]_n$ (**7**) was isolated by hydrothermal reactions and characterized magnetically. Research results also show the frequency dependence of AC magnetic susceptibilities, although the phthalate anions mediate antiferromagnetic coupling between Dy^{III} ions. Further magnetic investigation of a neutral mononuclear complex with the formula $[Dy(TTA)_3(L_3)]$ (**8**) (TTA = 2-thenoyltrifluoroacetonate; L_3 = 4,5-pinene bipyridine) suggests that the single-ion magnetic behavior originates the slow relaxation of Dy^{III}-containing complexes.

Introduction

In the past decade, low-dimensional magnets including single-molecule magnets (SMMs)[1] and single-chain magnets (SCMs)[2] have attracted considerable attention of both physicists and chemists because of their slow magnetic relaxation. Many interesting features of low-dimensional magnets such as magnetic hysteresis behavior,[3a] quantum tunneling of magnetization,[3b,c] and quantum interference effects[3d] were attributed to this kind of magnetic behavior. Therefore, the slow magnetic relaxation process has become a very important characterization for judging low-dimensional magnets when Glauber's theory as the main method is used to explain its slow dynamics of magnetization.[2a,3e]

Within the many characteristics required in chemical design of low-dimensional magnets, one important factor concerns the strong magnetic anisotropy[1d] of clusters or chains, which provides an energy barrier for reversal of magnetization and is the determinant importance for getting convenient relaxation time. In the synthesis of low-dimensional magnets, magnetic anisotropy relating to magnetocrystalline anisotropy and coupling anisotropy is hard to be tuned, but the metal ions with significant anisotropy can be chosen easily. Usually, Co^{II}, Mn^{III}, and low-spin Fe^{III} ions in the first-row transition metals (M), and lanthanide (Ln) ions except Gd^{III}, are the promising candidates in the design of low-dimensional magnets. To date, many reported lanthanide complexes show low-dimensional

*To whom correspondence should be addressed. E-mail: yousong@nju.edu.cn (Y.S.), youxz@nju.edu.cn (X.-Z.Y.).

(1) (a) Gatteschi, D.; Caneschi, A.; Pardi, L.; Sessoli, R. *Science* **1994**, *265*, 1054. (b) *Magnetism: Molecules to Materials*; Miller, J. S., Drillon, M., Eds.; Wiley-VCH: Weinheim, Germany, 2001−2004; Vols. *1*−*4*. (c) Wernsdorfer, W.; Aliaga-Alcalde, N.; Hendrickson, D. N.; Christou, G. *Nature* **2002**, *416*, 406. (d) Gatteschi, D.; Sessoli, R. *Angew. Chem., Int. Ed.* **2003**, *42*, 268. (e) Gatteschi, D.; Sessoli, R. *Angew. Chem., Int. Ed.* **2003**, *42*, 268. (f) Tasiopoulos, A. J.; Vinslava, A.; Wernsdorfer, W.; Abboud, K. A.; Christou, G. *Angew. Chem., Int. Ed.* **2004**, *43*, 2117. (g) Song, Y.; Zhang, P.; Ren, X.-M.; Shen, X.-F.; Li, Y.-Z.; You, X.-Z. *J. Am. Chem. Soc.* **2005**, *127*, 3708. (h) Aromí, G.; Brechin, E. K. *Struct. Bonding* (*Berlin*) **2006**, *122*, 1 and references therein. (i) Ako, A. M.; Hewitt, I. J.; Mereacre, V.; Clérac, R.; Wernsdorfer, W.; Anson, C. E.; Powell, A. K. *Angew. Chem., Int. Ed.* **2006**, *45*, 4926. (j) Schelter, E. J.; Karadas, F.; Avendano, C.; Prosvirin, A. V.; Wernsdorfer, W.; Dunbar, K. R. *J. Am. Chem. Soc.* **2007**, *129*, 8139.

(2) (a) Caneschi, A.; Gatteschi, D.; Lalioti, N.; Sangregorio, C.; Sessoli, R.; Venturi, G.; Vindigni, A.; Rettori, A.; Pini, M. G.; Novak, M. A. *Angew. Chem., Int. Ed.* **2001**, *40*, 1760. (b) Clérac, R.; Miyasaka, H.; Yamashita, M.; Coulon, C. *J. Am. Chem. Soc.* **2002**, *124*, 12837. (c) Lescoüzec, R.; Vaissermann, J.; Ruiz-Pérez, C.; Lloret, F.; Carrasco, R.; Julve, M.; Verdaguer, M.; Dromzee, Y.; Gatteschi, D.; Wernsdorfer, W. *Angew. Chem., Int. Ed.* **2003**, *42*, 1483. (d) Liu, T.-F.; Fu, D.; Gao, S.; Zhang, Y.-Z.; Sun, H.-L.; Su, G.; Liu, Y.-J. *J. Am. Chem. Soc.* **2003**, *125*, 13976. (e) Wang, S.; Zuo, J.-L.; Gao, S.; Song, Y.; Zhou, H.-C.; Zhang, Y.-Z.; You, X.-Z. *J. Am. Chem. Soc.* **2004**, *126*, 8900–8902. (f) Bai, Y.-L.; Tao, J.; Wernsdorfer, W.; Sato, O.; Huang, R.-B.; Zheng, L.-S. *J. Am. Chem. Soc.* **2006**, *128*, 16428.

(3) (a) Sessoli, R.; Gatteschi, D.; Caneschi, A.; Novak, M. A. *Nature* **1993**, *365*, 141. (b) Thomas, L.; Lionti, F.; Ballou, R.; Gatteschi, D.; Sessoli, R.; Barbara, B. *Nature* **1996**, *383*, 145. (c) Friedman, J. R.; Sarachik, M. P.; Tejada, J.; Ziolo, R. *Phys. Rev. Lett.* **1996**, *76*, 3830. (d) Wernsdorfer, W.; Sessoli, R. *Science* **1999**, *284*, 133. (e) Glauber, R. J. *J. Math. Phys.* **1963**, *4*, 294.

Published on Web 12/29/2009

magnetic properties, mainly including M-Ln bimetallic[4a−q] and Ln-radical[4r,s] assemblies. Pure lanthanide complexes are fewer reported.[4t,v] Even mononuclear complexes display slow magnetic relaxation.[5] Noticeably, most lanthanide SMMs and SCMs contain Dy^{III} ion, strongly indicating the f electrons of Dy^{III} ion may provide different magnetic contributions from other Ln^{III} ions. For investigating the origin of slow magnetic relaxation in Dy^{III}-based complexes, a series of one-dimensional (1D) Ln^{III} chains, a two-dimensional (2D) layer, and a mononuclear Dy^{III} complex were synthesized and characterized magnetically. Experimental results indicate that the slow relaxation of magnetization may be ascribed to the single-ion behavior of Dy^{III}. Herein, we report the preparations, crystal structures, and magnetic properties of a series of 1D chains, $[Ln(L_1)_3(HOCH_2CH_2OH)]_n$ (L_1 = 2-furoate anion; Ln = Nd (**1**), Sm (**2**), Gd (**3**), Tb (**4**), Dy (**5**), Er (**6**)), a 2D layer $[Dy_2(L_2)_6(H_2O)]_n$ (**7**) (L_2 = phthalate anion) and a mononuclear complex $[Dy(TTA)_3(L_3)]$ (**8**) (TTA = 2-thenoyltrifluoroacetonate; L_3 = 4,5-pinene bipyridine).

Experimental Section

Materials and Methods. All of the chemicals were purchased from commercial suppliers and were used without further purification. Elemental analyses for carbon, hydrogen were carried out with a Perkin-Elmer 240C elemental analyzer. X-ray single crystal diffraction was carried out on a Bruker SMART Apex II CCD-based diffractometer at room temperature.

Magnetic Measurements. All magnetization data were recorded on a Quantum Design MPMS-XL7 SQUID magnetometer. The variable-temperature magnetization was measured with an external magnetic field of 100 Oe in the temperature range of 1.8−300 K. The experimental magnetic susceptibility data are corrected for the diamagnetism estimated from Pascal's tables and sample holder calibration. The lanthanide ions usually have strongly magnetic anisotropy, which may lead to the polycrystalline aligning along the external field in the measurement. Therefore, all magnetic measurements were carried out in our experiments according to following procedure. A selected large single crystal sample (for purity) was crushed into a polycrystalline sample. The polycrystalline sample was packed in a viscid film, and a suitable pressure was applied to compress the small packet with sample in a compaction to ensure that the polycrystalline sample stay unmoved. And then, the prepared sample package was fixed in a straw and installed into the SQUID chamber.

X-ray Crystallography. X-ray single crystal diffraction measurements of the title complexes were carried out on a SMART CCD area detector equipped with a graphite crystal monochromator situated in the incident beam for data collection at 293(2) K. The structures were solved by direct methods and refined with full-matrix least-squares techniques using SHELXS-97 and SHELXL-97 programs.[6,7] Anisotropic thermal parameters were assigned to all H atoms. Selected bond lengths and angles for the title complexes are listed in Supporting Information, Tables S1 and S2, respectively.

Synthesis of $[Ln(L_1)_3(HOCH_2CH_2OH)]_n$ (Ln = Nd (1), Sm(2), Gd(3), Tb(4), Dy (5), Er(6)). A mixture of $Ln(NO_3)_3\cdot 6H_2O$ (0.1 mmol) and L_1 (0.1 mmol) was stirred for 0.5 h in distilled water (20 mL) and $HOCH_2CH_2OH$ (5 mL). The pH value was adjusted to about 7 with dilute aqueous NaOH. Upon slow evaporation of the filtrate at room temperature for 2 weeks, well-shaped crystals suitable for X-ray single crystal diffraction were obtained. Yield (%): 56 for **1**, 62 for **2**, 59 for **3**, 65 for **4**, 66 for **5**, 54 for **6**, based on lanthanide salts. Elemental analysis calcd (%) for **1** ($C_{17}H_{15}O_{11}Nd$, 539.53): C 37.85, H 2.80; found: C 37.47, H 2.55. For **2** ($C_{17}H_{15}O_{11}Sm$, 545.65): C 37.42, H 2.77; found: C 37.26, H 2.84. For **3** ($C_{17}H_{15}O_{11}Gd$, 552.54): C 36.95, H 2.74; found: C 36.69, H 3.01. For **4** ($C_{17}H_{15}O_{11}Tb$, 554.22): C 36.84, H 2.73; found: C 37.19, H 2.49. For **5** ($C_{17}H_{15}O_{11}Dy$, 557.79): C 36.61, H 2.71; found: C 36.25, H 2.49. For **6** ($C_{17}H_{15}O_{11}Er$, 562.55): C 36.30, H 2.69; found: C 36.02, H 2.82.

Synthesis of $[Dy_2(L_2)_6(H_2O)]_n$ (7). A mixture of $Dy(NO_3)_3\cdot 6H_2O$ (0.1 mmol), 1,10-phenanthroline (0.1 mmol), L_2 (0.1 mmol), and H_2O (12 mL) was put in a 20 mL acid digestion bomb and heated at 160 °C for 3 days. The crystal products were collected after washed with H_2O (2 × 5 mL). Yield (%): 40, based on $Dy(NO_3)_3\cdot 6H_2O$. Elemental analysis calcd (%) for **7** ($C_{24}H_{14}Dy_2O_{13}$, 835.36): C, 34.51; H, 1.69. Found: C, 34.26; H, 1.58.

Synthesis of $[Dy(TTA)_3(L_3)]$ (8). The preparation of **8** was carried out using a procedure similar to that employed of $Eu(TTA)_3(L_3)$.[8] Yield (%): 60, based on $Dy(NO_3)_3\cdot 6H_2O$. Elemental analysis calcd for **8** ($C_{41}H_{30}N_2O_6F_9S_3Dy$, 1076.38): C, 45.75; H, 2.81; N, 2.60. Found: C, 45.96; H, 2.90; N, 2.83.

Results and Discussion

Structural Descriptions of Complexes 1−8. The structures of **1**−**8** were determined by single-crystal X-ray diffraction analysis (Table 1). Selected bond lengths and angles for **1**−**8** are listed in Supporting Information, Table S1.

(4) (a) Mereacre, V. M.; Ako, A. M.; Clérac, R.; Wernsdorfer, W.; Filoti, G.; Bartolomé, J.; Anson, C. E.; Powell, A. K. *J. Am. Chem. Soc.* **2007**, *129*, 9248. (b) Mishra, A.; Tasiopoulos, A. J.; Wernsdorfer, W.; Moushi, E. E.; Moulton, B.; Zaworotko, M. J.; Abboud, K. A.; Christou, G. *Inorg. Chem.* **2008**, *47*, 4832. (c) Chandrasekhar, V.; Pandian, B. M.; Azhakar, R.; Vittal, J. J.; Clérac, R. *Inorg. Chem.* **2007**, *46*, 5140. (d) Mereacre, V.; Ako, A. M.; Clérac, R.; Wernsdorfer, W.; Hewitt, I. J.; Anson, C. E.; Powell, A. K. *Chem.—Eur. J.* **2008**, *14*, 3577. (e) Mishra, A.; Wernsdorfer, W.; Abboud, K. A.; Christou, G. *J. Am. Chem. Soc.* **2004**, *126*, 15648. (f) Chandrasekhar, V.; Pandian, B. M.; Boomishankar, R.; Steiner, A.; Vittal, J. J.; Houri, A.; Clérac, R. *Inorg. Chem.* **2008**, *47*, 4918. (g) Zaleski, C. M.; Depperman, E. C.; Kampf, J. W.; Kirk, M. L.; Pecoraro, V. *Angew. Chem., Int. Ed.* **2004**, *43*, 3912. (h) Zaleski, C. M.; Kampf, J. W.; Mallah, T.; Kirk, M. L.; Pecoraro, V. L. *Inorg. Chem.* **2007**, *46*, 1954. (i) Zaleski, C. M.; Depperman, E. C.; Kampf, J. W.; Kirk, M. L.; Pecoraro, V. *Inorg. Chem.* **2006**, *45*, 10022. (j) Costes, J.-P.; Shova, S.; Wernsdorfer, W. *Dalton Trans.* **2008**, 1843. (k) Pointillart, F.; Bernot, K.; Sessoli, R.; Gatteschi, D. *Chem.—Eur. J.* **2007**, *13*, 1602. (l) Mori, F.; Nyui, T.; Ishida, T.; Nogami, T.; Choi, K.-Y.; Nojiri, H. *J. Am. Chem. Soc.* **2006**, *128*, 1440. (m) Aronica, C.; Pilet, G.; Chastanet, G.; Wernsdorfer, W.; Jacquot, J.-P.; Luneau, D. *Angew. Chem., Int. Ed.* **2006**, *45*, 4659. (n) Ferbinteanu, M.; Kajiwara, T.; Choi, K.-Y.; Nojiri, H.; Nakamoto, A.; Kojima, N.; Cimpoesu, F.; Fujimura, Y.; Takaishi, S.; Yamashita, M. *J. Am. Chem. Soc.* **2006**, *128*, 9008. (o) Osa, S.; Kido, T.; Matsumoto, N.; Re, N.; Pochaba, A.; Mrozinski, J. *J. Am. Chem. Soc.* **2004**, *126*, 420. (p) Costes, J.-P.; Dahan, F.; Wernsdorfer, W. *Inorg. Chem.* **2006**, *45*, 5. (q) Costes, J.-P.; Clemente-Juan, J. M.; Dahan, F.; Milon, J. *Inorg. Chem.* **2004**, *43*, 8200. (r) Bogani, L.; Sangregorio, C.; Sessoli, R.; Gatteschi, D. *Angew. Chem., Int. Ed.* **2005**, *44*, 5817. (s) Bernot, K.; Bogani, L.; Caneschi, A.; Gatteschi, D.; Sessoli, R. *J. Am. Chem. Soc.* **2006**, *128*, 7947. (t) Tang, J.; Hewitt, I.; Madhu, N. T.; Chastanet, G.; Wernsdorfer, W.; Ansen, C. E.; Benelli, C.; Sessoli, R.; Powell, A. K. *Angew. Chem., Int. Ed.* **2006**, *45*, 1729. (u) Gamer, M. T.; Lan, Y.; Roesky, P. W.; Powell, A. K.; Clérac, R. *Inorg. Chem.* **2008**, *47*, 6581. (v) Lin, P.-H.; Burchell, T. J.; Clérac, R.; Murugesu, M. *Angew. Chem., Int. Ed.* **2008**, *47*, 8848.

(5) (a) Ishikawa, N. *Polyhedron* **2007**, *26*, 2147. (b) Ishikawa, N.; Sugita, M.; Wernsdorfer, W. *J. Am. Chem. Soc.* **2005**, *127*, 3650. (c) Ishikawa, N.; Sugita, M.; Wernsdorfer, W. *Angew. Chem., Int. Ed.* **2005**, *44*, 2931. (d) Ishikawa, N.; Sugita, M.; Ishikawa, T.; Koshihara, S.; Kaizu, Y. *J. Am. Chem. Soc.* **2003**, *125*, 8694. (e) Ishikawa, N.; Sugita, M.; Tanaka, N.; Ishikawa, T.; Koshihara, S.; Kaizu, Y. *Inorg. Chem.* **2004**, *43*, 5498. (f) AlDamen, M. A.; Clemente-Juan, J. M.; Coronado, E.; Martí-Gastaldo, C.; Gaita-Ariño, A. *J. Am. Chem. Soc.* **2008**, *130*, 8874.

(6) Sheldrick, G. M. *SHELXS 97, Program for the Solution of Crystal Structures*; University of Göttingen: Göttingen, Germany, 1997.

(7) Sheldrick, G. M. *SHELXL 97, Program for the Refinement of Crystal Structures*; University of Göttingen: Göttingen, Germany, 1997.

(8) (a) Li, X.-L.; Chen, K.; Liu, Y.; Wang, Z.-X.; Wang, T.-W.; Zuo, J.-L.; Li, Y.-Z.; Wang, Y.; Zhu, J. S.; Liu, J.-M.; Song, Y.; You, X.-Z. *Angew. Chem., Int. Ed.* **2007**, *46*, 6820. (b) Li, X.-L.; Zhen, Y.; Zuo, J.-L.; Song, Y.; You, X.-Z. *Polyhedron* **2007**, *26*, 5257.

Table 1. X-ray Crystallographic Data for Complexes **1**−**8**

	1	**2**	**3**	**4**	**5**	**6**	**7**	**8**
chemical formula	$C_{17}H_{15}O_{11}Nd$	$C_{17}H_{15}O_{11}Sm$	$C_{17}H_{15}O_{11}Gd$	$C_{17}H_{15}O_{11}Tb$	$C_{17}H_{15}O_{11}Dy$	$C_{17}H_{15}O_{11}Er$	$C_{24}H_{14}Dy_2O_{13}$	$C_{41}H_{30}DyF_9N_2O_6S_3$
fw	539.53	545.64	552.54	554.22	557.79	562.55	835.35	1076.35
crystal system	monoclinic	monoclinic	monoclinic	monoclinic	monoclinic	monoclinic	monoclinic	monoclinic
space group	*P*2(1)/*c*	*P*2(1)/*c*	*P*2(1)/*c*	*P*2(1)/*c*	*P*2(1)/*c*	*P*2(1)/*c*	*P*2(1)/*c*	*P*2(1)
a (Å)	9.6325(2)	9.6717(10)	9.6811(7)	9.6649(5)	9.6699(19)	9.6516(10)	7.9241(4)	10.1909(19)
b (Å)	19.3591(5)	19.445(2)	19.3670(15)	19.3404(10)	19.337(4)	19.2802(19)	26.3867(15)	19.015(4)
c (Å)	11.2552(3)	11.2537(12)	11.2416(8)	11.2354(6)	11.235(2)	11.1986(11)	11.5784(6)	12.082(2)
β (deg)	111.1090(10)	111.2680(10)	111.3180(10)	111.3480(10)	111.296(9)	111.4500(10)	106.8510(10)	113.902(4)
V/Å^3	1957.99(8)	1972.3(4)	1963.5(3)	1956.06(18)	1957.3(6)	1939.6(3)	2317.0(2)	2140.4(7)
Z	4	4	4	4	4	4	4	2
D/g cm^{-3}	1.830	1.838	1.869	1.882	1.893	1.926	2.395	1.670
μ/mm^{-1}]	2.709	3.034	3.435	3.673	3.875	4.385	6.475	1.979
reflections measured/unique	18185/4504	17000/4529	16919/4529	12132/4656	18889/4447	16825/4483	11604/4076	9777/6289
data with ($I > 2\sigma(I)$)	4091	4045	4145	3188	3081	3541	3820	5288
R^a/wR^b	0.0382/0.0837	0.0293/0.0690	0.0280/0.0631	0.0447/0.0878	0.0573/0.1048	0.0270/0.0831	0.0502/0.1364	0.0635/0.0963

$^a R = \sum||F_o| - |F_c||/\sum|F_o|$. $^b R_w = [\sum w(F_o^2 - F_c^2)^2/\sum w(F_o^2)^2]^{1/2}$.

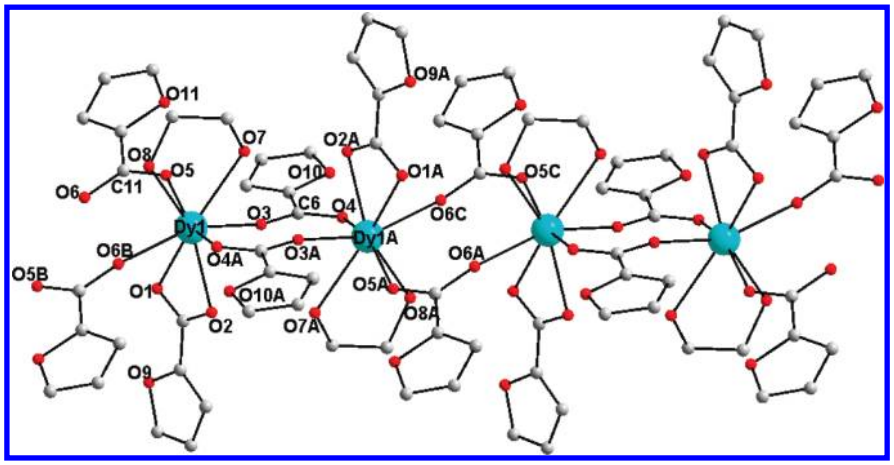

Figure 1. 1D alternative chain of **5** along *b* axis. Cyan, Dy; red, O; gray, C.

X-ray structure analysis shows that complexes **1**−**6** are isomorphous (Table 1), so only the structure of **5** is described typically. In **5**, the asymmetric unit contains one independent Dy^{III} ion, three 2-furoate anions, and one bidentate-chelated glycol molecule. Dy^{III} ion is situated in an extremely asymmetric eight-coordinated environment, so that its geometry can be hardly determined as a known polyhedron. It can be roughly regarded as a distorted bicapped trigonal prism (Supporting Information, Figure S1). As illustrated as Figure 1, a η^2-$HOCH_2CH_2OH$ molecule and a η^2-2-furoate anion chelate Dy^{III} ion are in a *trans*-mode, while the neighboring Dy^{III} ions are bridged by four *syn-anti* 2-furoate anions in pairs by μ_2-O3-C6-O4 and μ_2-O5-C11-O6 carboxylates to form a 1D alternative chain along the *b* axis. The packing view along the *a* axis displayed in Supporting Information, Figure S2 clearly shows these separating chains. The separation of two neighboring Dy^{III} ions within the chain is 4.783 and 4.911 Å, and the shortest distance of Dy^{III} ions between chains is 9.670 Å. Comparisons of local environments of Ln^{III} ions in other lanthanide complexes are summarized in Supporting Information, Table S2.

For comparing the following magnetic properties, complex **7** with different structure from the literature compound was synthesized by substituting $Dy(NO_3)_3 \cdot 6H_2O$ for reactant of $LnCl_3 \cdot 6H_2O$.[9] Complex **7** is a neutral 2D coordination polymer, and the second building unit (SBU, Figure 2) consists of two Dy^{III} centers, one water, and three phthalate ligands with three coordination modes (Scheme 1). Both Dy1 and Dy2 are eight-coordinated. Dy1 is coordinated by one water molecule and seven carboxylates from five phthalate anions. The coordination geometry can be viewed as a slightly distorted dodecahedron because multicarboxylates coordinate to Dy1 and the donor oxygen atoms equably distribute around Dy1 (Supporting Information, Figure S3a). In contrast, Dy2 is coordinated by eight carboxyl oxygen atoms from six phthalate ligands, of which two carboxyl groups provide all oxygen atoms coordinating to Dy2. So the coordination environment displays a very low symmetry just like those of **1**−**6**, viewed as a strongly distorted bicapped trigonal prism (Supporting Information, Figure S3b). O6, O12A, and O3 from three carboxyl groups bridge Dy1 and Dy2, one of which is in *syn-anti* bridging configuration. The adjacent SBUs are connected by carboxyl bridges in *mono*- and *bidentate*- mode into a 2D-layered motif. The shortest Dy···Dy separation in

(9) Wang, Y.-H.; Jin, L.-P.; Wang, K.-Z. *J. Mol. Struct.* **2003**, *649*, 85.

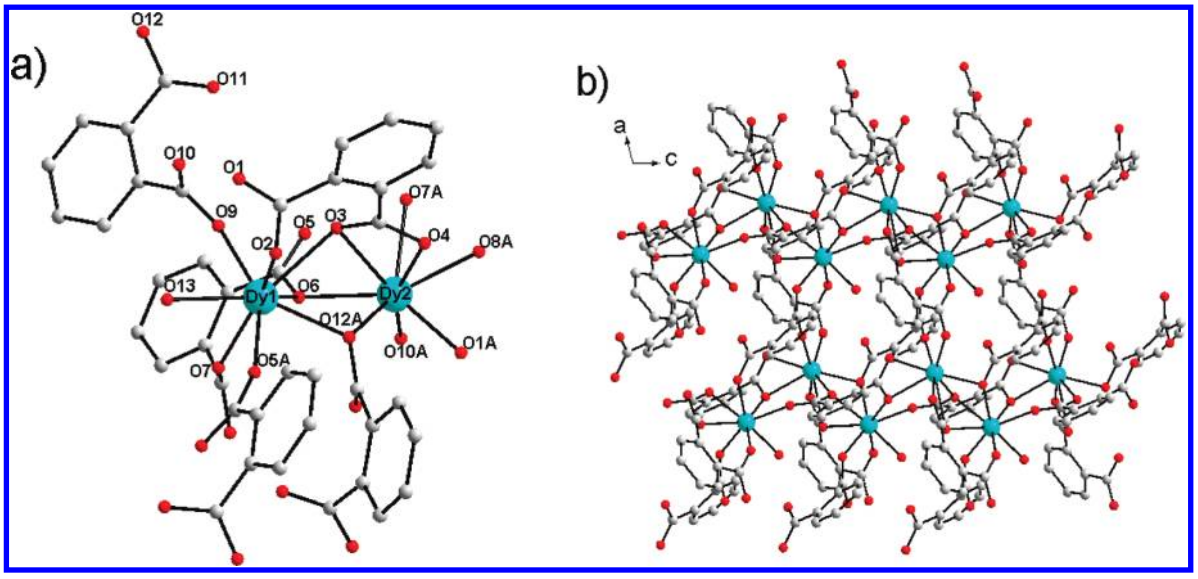

Figure 2. Dinuclear Dy_2 coordination unit of **7** for (a) and view of a 2D layer along *b* axis for (b). Cyan, Dy; red, O; gray, C.

Scheme 1. Coordination Modes of Phthalic Ligands in **7**[a]

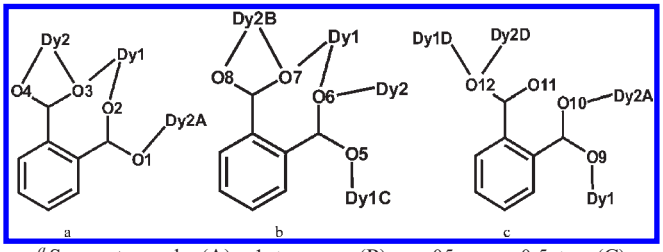

[a] Symmetry code: (A) $-1+x, y, z$; (B) $x, -05-y, -0.5+z$; (C) $x, -05-y, -1.5+z$; (D) $-1+x, -05-y, -1.5+z$.

the dinuclear unit and between the neighboring SBUs are 3.725 and 4.412 Å, respectively.

The structure of **8** is almost the same as that in our previous work (Figure 3).[8] Complex **8** crystallizes in a chiral space group $P2_1$, owing to the presence of the chiral bipyridine derivative. The chirality of **8** is dominated by the two chiral centers (C37 and C38) of the bipyridine derivative. As shown in Figure 3, the Dy^{III} ion is surrounded by six oxygen atoms from three TTA ligands and two nitrogen atoms of (+)-4,5-pinene bipyridine. The geometry of O_6N_2 donor set can be best approximated as a distorted square antiprism, as illustrated in Supporting Information, Figure S4. The distances of Dy−O are in the range of 2.334−2.383 Å and the Dy−N bond lengths are 2.558 and 2.566 Å, respectively, all being normal coordination bonds. The O1−O2−O3-O4 (bottom plane) and O5−O6−N1−N2 atoms (top plane) comprise the two square-basic planes of the antiprism with mean deviations of 0.0342 and 0.0308 Å from each plane, and their dihedral angle is 3.6°. Two square planes are unparallel to each other, and the top plane is rotated by only a smaller angle of 21.1° from the bottom plane than the angle of 45° for a regular square antiprism. One of the thienyl rings in the three β-diketonate anions is disordered on S2 and C11 atoms.

Magnetic Properties. Temperature-dependent magnetic susceptibility measurements for **1**−**8** were performed on the polycrystalline samples in the range of 300−1.8 K under 100 Oe of external field (Figure 4 and Supporting Information, Figures S5−S9). The magnetic properties of **3** were discussed at first because of no orbital contribution in the Gd^{III}-based complex. For **3**, $\chi_M T$ almost remains a constant from 7.86 cm^3 K mol^{-1} at 300 K to 7.74 cm^3 K mol^{-1} at 26 K (Figure 4a), which is consistent with the spin-only value of 7.88 cm^3 K mol^{-1} based on a Gd^{III} ion. Upon further cooling, the $\chi_M T$ versus T curve exhibits a sharp but very small decrease below 10 K, and $\chi_M T$ reaches to 7.15 cm^3 K mol^{-1} at 1.8 K. This feature indicates the presence of very weak antiferromagnetic interaction between Gd^{III} ions. In **3**, carboxyl group of 2-furoate bridges two adjacent Gd^{III} ions in a *syn-anti* mode forming an alternative chain, so the chain model can be used here to estimate the magnetic exchange interaction.[10a] The best fitting results (Figure 4a), based on either alternative or uniform chain model, gave: $g_J = 1.994$, $J_1 = J_2 = -0.006(1)$ cm^{-1} and $R = 8.9 \times 10^{-4}$ ($R = \sum[(\chi_M T)_{calc} - (\chi_M T)_{obs}]^2/\sum(\chi_M T)_{obs}^2$), where J_1 and J_2 are the coupling constants within chain. The results indicate that the magnetic coupling between Gd^{III} ions mediated by *syn-anti* carboxyl bridges is very weak. A spin density functional calculation result shows such a small coupling constant is not significantly different from zero in its effect on the magnetic properties.[10b] Actually, complex **3** almost shows a paramagnetic behavior.

Although complexes **1**, **2**, **4**, **5**, and **6** are isomorphous with **3**, they exhibit different magnetic properties because of the significant orbital contributions of Ln^{III} ions. It is known that in lanthanide complexes, the spin−orbital coupling leads to the $4f^n$ configuration splitting into $^{2S+1}L_J$ states, and finally into Stark components under the ligand-field (LF) perturbation.[11] So the variable-temperature magnetic properties of a free Ln^{III} ion generally strongly deviate from the Curie law, and $\chi_M T$ decreases with the system cooling because of the depopulation of Stark levels. However, small crystal-field effects above room temperature do

(10) (a) Cortés, R.; Drillon, M.; Solans, X.; Lezama, L.; Rojo, T. *Inorg. Chem.* **1997**, *36*, 677. (b) Roy, L. E.; Hughbanks, T. *J. Am. Chem. Soc.* **2006**, *128*, 568 and references therein.

(11) (a) Bünzli, J.-C. G.; Chopin, G. R. *Lanthanide Probes in Life, Chemical and Earth Sciences: Theory and Practice*; Elsevier: Amsterdam, The Netherlands, 1989. (b) Costes, J.-P.; Nicodème, F. *Chem.—Eur. J.* **2002**, *8*, 3442. (c) Benelli, C.; Gatteschi, D. *Chem. Rev.* **2002**, *102*, 2369.

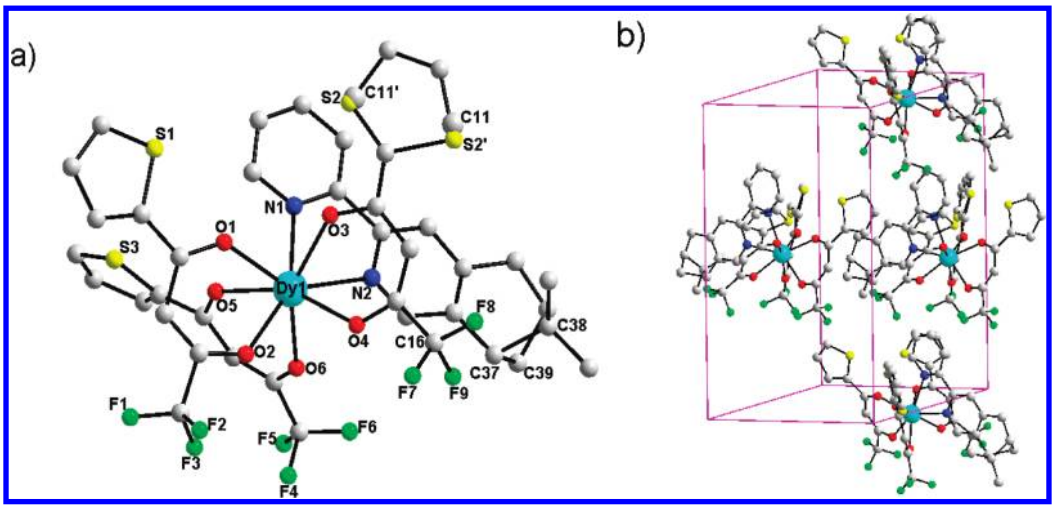

Figure 3. Mononuclear structure for (a) and the unit packing arrangement of **8** for (b). Cyan, Dy; red, O; gray, C; green, F; blue, N; yellow, S; purple line, unit cell.

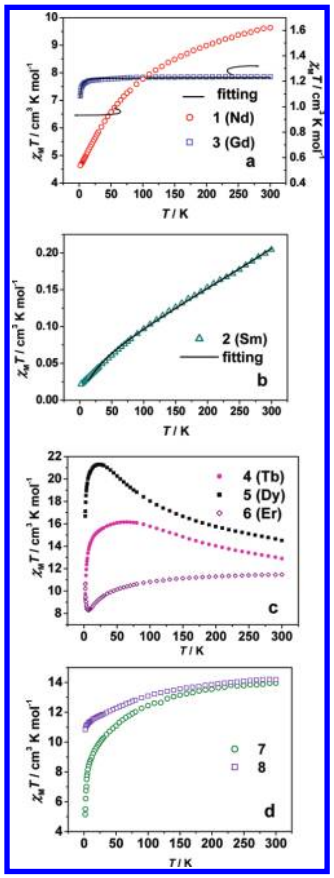

Figure 4. Temperature dependence of magnetic susceptibilities of (a): **1** (Nd: ○) and **3** (Gd: □); (b) **2** (Sm: Δ); (c) **4** (Tb: ●), **5** (Dy: ■) and **6** (Er: ◊); (d) **7** (olive) and **8** (violet) in the forms of $\chi_M T$.

not result in this kind of deviation from the paramagnetic properties of Ln^{III} ions.

For **1**, $\chi_M T$ is 1.62 cm^3 K mol^{-1} at 300 K, slightly lower than the theoretical value of 1.64 cm^3 K mol^{-1} per insulated Nd^{III} ion in the $^4I_{9/2}$ ground state (g = 8/11).

(12) (a) Andruh, M.; Bakalbassis, E.; Kahn, O.; Trombe, J. C.; Porcher, P. *Inorg. Chem.* **1993**, *32*, 1616. (b) Wang, Z.-X.; Shen, X.-F.; Wang, J.; Zhang, P.; Li, Y.-Z.; Nfor, E. N.; Song, Y.; Ohkoshi, S.; Hashimoto, K.; You, X.-Z. *Angew. Chem., Int. Ed.* **2006**, *45*, 3287.

Upon further cooling, $\chi_M T$ decreases monotonically as expected for the spin−orbital coupling (Figure 4a). However, $\chi_M T$ of 0.54 cm^3 K mol^{-1} at 1.8 K is lower than the single-ion value in literature,[12] suggesting antiferromagnetic spin−spin coupling between Nd^{III} ions, accompanied with spin−orbital coupling.

The plot of $\chi_M T$ versus T for **2** is similar to that of **1** with $\chi_M T$ of 0.20 cm^3 K mol^{-1} at 300 K and 0.022 cm^3 K mol^{-1} at 1.8 K (Figure 4b). According to the treatment of single-ion Sm^{III} by Kahn,[12a] the intrachain coupling constant between Sm^{III} can be roughly estimated by the mean-field theory as follows:

$$\chi_{Sm} = (N\beta^2/3kTx)[2.143x + 7.347 + (42.92x + 1.641)e^{-7x/2} + (283.7x - 0.6571)e^{-8x} + (620.6x - 1.94)e^{-27x/2} + (1122x - 2.835)e^{-20x} + (1813x - 3.556)e^{-55x/2}]/(3 + 4e^{-7x/2} + 5e^{-8x} + 6e^{-27x/2} + 7e^{-20} + 8e^{-55x/2})$$

$$\chi_M = \chi_{Sm}/[1 - (2zj'/Ng_J\beta^2)\chi_{Sm}]$$

where $x = \lambda/kT$, λ is the spin−orbit coupling parameter, g_J is the Landé factor, and zj' is the coupling interaction between Sm^{III} ions within chain. The best fitting results gave: g_J = 0.289, λ = 347, and zj' = −4.0 cm^{-1} with R = 3.1 × 10^{-6}. The calculated g_J is very close to the theoretical value of 2/7 and the negative value of zj' indicates the weak antiferromagnetic coupling between Sm^{III} ions in **2**.

For **4**, $\chi_M T$ slowly increases from 12.90 cm^3 K mol^{-1} at 300 K (theoretical value is 11.82 cm^3 K mol^{-1} based on a non-interacted Tb^{III} ion of the $^7F_6$ ground state with g = 3/2) to 16.14 cm^3 K mol^{-1} at 70 K. Upon cooling, $\chi_M T$ decreases to 9.26 cm^3 K mol^{-1} at 1.8 K. The $\chi_M T$ versus T curve shows a broad protuberance around 70 K (Figure 4c), indicating the presence of ferromagnetic interaction between Tb^{III} ions, and this kind of interaction is strong enough to compensate the decrease of $\chi_M T$ resulted from the depopulated Stark states. However, the variable-field data do not provide the evidence of

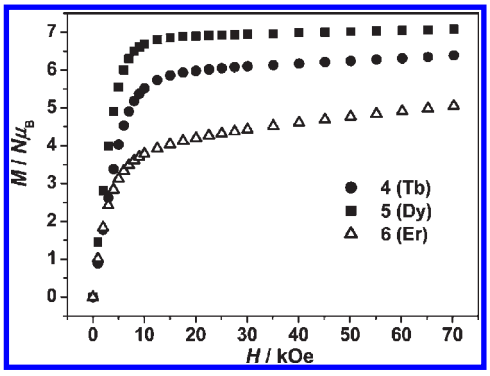

Figure 5. Field dependence of magnetizations of **4** (Tb: ●), **5** (Dy: ■), and **6** (Er: Δ) at 1.8 K.

ferromagnetic coupling because of the considerable LF effects at low temperature, leading to a lower magnetization (6.38 $N\mu_B$) than theoretical value ($g_J \times J = 3/2 \times 6 = 9\ N\mu_B$) under 70 kOe (Figure 5). It can be explained that the depopulation of the Stark levels of the Ln^{III} $^{2S+1}L_J$ ground state under the LF perturbation produces a much smaller effective spin (even reaches $S = 1/2$),[12a] especially in the low temperature region, which results in a lower gS value of magnetic moment with strong uniaxial Ising-type anisotropy of the g tensor.[4t,u,13] The ferromagnetic interaction leading to the increase in $\chi_M T$ products with cooling may be ascribed to the dipole−dipole interaction between Ln^{III} ions,[13a] suggesting that the spin polarization effect in the three-atom bridge may induce the parallel arrangement of spins in neighboring magnetic centers.

As depicted in Figure 4c, complex **5** shows similar magnetic properties with **4**. The room-temperature and maximum values of $\chi_M T$ are 14.50 and 21.30 $cm^3\ K\ mol^{-1}$ (at 22 K), respectively. It is believed that the short-range interaction between Dy^{III} ions is stronger than that between Tb^{III} ions because $\chi_M T$ of **5** increases more quickly than that of **4** with the temperature cooling.

Complex **6** shows a different plot of $\chi_M T$ versus T from others, in which $\chi_M T$ slowly decreases from 11.46 $cm^3\ K\ mol^{-1}$ at 300 K to a minimum of 8.30 $cm^3\ K\ mol^{-1}$ at 7 K, and then sharply increases below 7 K (Figure 4c). This behavior accounts for the competition between spin−orbital coupling of single-ion Er^{III} and ferromagnetic interaction within the chain. Above 7 K, the former effect dominates the magnetic properties, while below 7 K the latter overcomes the orbital contribution of Er^{III} ion and compensates the decrease of $\chi_M T$. This phenomenon was also observed in other compounds showing ferromagnetic interaction between Ln^{III} ions.[14]

Similar to the properties of **4**, the ferromagnetic interaction between Ln^{III} ions in **5** and **6** is not consistent

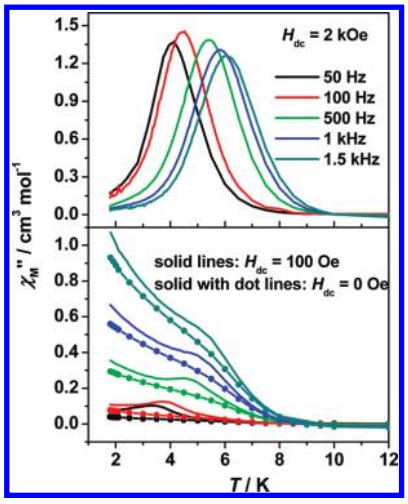

Figure 6. Temperature dependence of AC susceptibilities of out-of-phase for **5** in $H_{dc} = 0$, 100 Oe and 2 kOe with $H_{ac} = 5$ Oe.

with the variable-field magnetization (Figure 5). Above 15 kOe, the magnetization of **5** reaches saturation of 7.08 $N\mu_B$, lower than the theoretical value ($g_J \times J = 4/3 \times 15/2 = 10\ N\mu_B$), indicating a much smaller effective spin in **5**. For **6**, besides the lower saturation value observed, the magnetization slowly and linearly increases with the external field above 15 kOe, which may be attributed to the anisotropy of the polycrystalline sample.

There are few examples of ferromagnetic interaction between Ln^{III} ions in rare earth compounds reported to date.[4v,14,15] The ferromagnetic interaction and the chain-like structure of the complexes described above prompted us to investigate their alternating current (AC) magnetic properties. When the static field was zero, AC magnetic measurements of **5** show the frequency dependence of magnetic susceptibilities in out-of-phase, but no peak was observed (Figure 6). When the static field was in 100 Oe, the broad peaks were displayed, indicating there is the quantum tunnelling of the magnetization at zero field. To investigate the dynamic properties of the slow magnetic relaxation and obtain an effective energy barrier (U_{eff}) close to the theoretical one, a stronger field of 2 kOe was applied in AC measurements to give good peak shapes in both in- (Supporting Information, Figure S10) and out-of-phase (Figure 6). Especially, the signals strongly depend on the frequencies of the AC field, and the quantum tunnelling was quenched by a direct current (DC) field. These behaviors are the essential nature of slow magnetic relaxation for a chain-like complex.

Further evidence of slow magnetic relaxation was obtained from the dynamic studies of magnetic properties. The correlation between peak temperatures, T_Ps, and their corresponding frequencies can educe two linear plots of $1/T_P$ versus $\ln(2\pi f)$, where the peak temperatures were roughly read in Figure 6 at 100 Oe or obtained by Lorentz peak function fitting in 2 kOe, respectively. Both

(13) (a) Carlin, R. L. *Magnetochemistry*; Springer: Berlin, 1986; Chapter 9. (b) Loong, C.-K.; Soderholm, L.; Goodman, G. L.; Abraham, M. M.; Boatner, L. A. *Phys. Rev. B* **1993**, *48*, 6124. (c) Prins, F.; Pasca, E.; Jongh, L. J. de; Kooijman, H.; Spek, A. L.; Tanase, S. *Angew. Chem., Int. Ed.* **2007**, *46*, 6081. (d) Chelebaeva, E.; Larionova, J.; Guari, Y.; Ferreira, R. A. S.; Carlos, L. D.; Paz, F. A. A.; Trifonov, A.; Guérin, C. *Inorg. Chem.* **2008**, *47*, 775.

(14) (a) Costes, J.-P.; Clemente-Juan, J. M.; Dahan, F.; Nicodème, F.; Verelst, M. *Angew. Chem., Int. Ed.* **2002**, *41*, 323. (b) Ishikawa, N.; Iino, T.; Kaizu, Y. *J. Am. Chem. Soc.* **2002**, *124*, 11440. (c) Baggio, R.; Garland, M. T.; Peña, O.; Perec, M. *Inorg. Chim. Acta* **2005**, *358*, 2332. (d) Zhang, Z.-H.; Song, Y.; Okamura, T.; Hasegawa, Y.; Sun, W.-Y.; Ueyama, N. *Inorg. Chem.* **2006**, *45*, 2896.

(15) (a) Hernandez-Molina, M.; Ruiz-Perez, C.; Lopez, T.; Lloret, F.; Julve, M. *Inorg. Chem.* **2003**, *42*, 5456. (b) Hou, H.; Li, G.; Li, L.; Zhu, Y.; Meng, X.; Fan, Y. *Inorg. Chem.* **2003**, *42*, 428. (c) Zheng, X.-J.; Wang, Z.-M.; Gao, S.; Liao, F.-H.; Yan, C.-H.; Jin, L.-P. *Eur. J. Inorg. Chem.* **2004**, 2968. (d) Manna, S. C.; Zangrando, E.; Bencini, A.; Benelli, C.; Chaudhuri, N. R. *Inorg. Chem. Acta* **2006**, *45*, 9114. (e) Abbas, G.; Lan, Y.; Kostakis, G.; Anson, C. E.; Powell, A. K. *Inorg. Chem. Acta* **2008**, *361*, 3494.

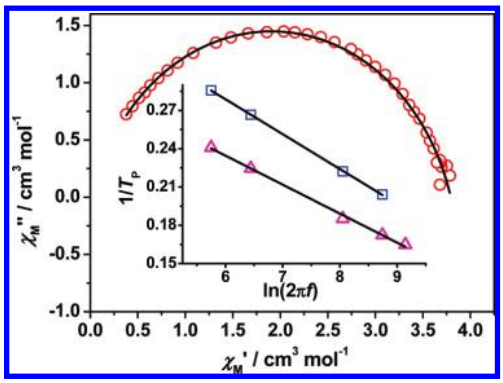

Figure 7. Cole−Cole diagram at 5 K for **5**. The solid line represents the fitting with a Debye model. Inset: Plots of $1/T_P$ vs $\ln(2\pi f)$ in H_{dc} = 100 Oe (□) and 2 kOe (△), respectively, and the fitting results by Arrhénius law (solid lines).

lines are in good agreement with the Arrhénius law, $1/T_P = -k_B/U_{eff} \times (\ln(2\pi f) + \ln(\tau_0))$ (inset in Figure 7). The best fitting results gave the relaxation time $\tau_0 = 9.3 \times 10^{-8}$ s and the energy barrier $U_{eff} = 36.6$ K in 100 Oe, and 8.1×10^{-8} s and 44.0 K in 2 kOe, respectively. All results *seem* consistent with lanthanide SCMs reported previously.[4r,s] It is suggested that the results in 2 kOe are closer to theoretical values because there still exists tunneling behavior in 100 Oe. At a fixed temperature of 5 K, a semicircle Cole−Cole diagram from 5 to 1500 Hz in 2 kOe (χ_M'' *versus* χ_M') was observed (Figure 7) and the least-squares fitting by a Debye model gave $\alpha = 0.17$, indicating the distribution of a single relaxation process in **5**.[16] However, surprisingly, ferromagnetic interaction between Ln^{III} ions in **4** and **6** does not cause frequency dependence of AC susceptibilities (Figures S13 and S14). To further investigate the unusual magnetic properties of Dy^{III}-based complexes, we randomly selected two samples without ferromagnetic coupling and characterized their magnetic properties.

Complex **7** is a 2D Dy^{III}-containing network. Variable-temperature magnetic properties were measured in the same conditions as that of **1**−**6**. As shown in Figure 4d, $\chi_M T$ continuously decreases from 13.96 cm^3 K mol^{-1} at 300 K to 8.53 cm^3 K mol^{-1} at 8 K based on one Dy^{III} ion. Below 8 K, $\chi_M T$ quickly goes down to 5.14 cm^3 K mol^{-1} at 1.8 K. This behavior is mainly attributed to the thermal depopulation of Stark components of the Dy^{III} $^6H_{15/2}$ ground state. However, comparing **7** with a noninteracting complex $\{Dy_2Zn_3\}_\infty$[17] in magnetic properties, we found that the $\chi_M T$ values of **7** is much lower than half $\chi_M T$ of $\{Dy_2Zn_3\}_\infty$ at low temperatures, indicating antiferromagnetic coupling between Dy^{III} ions in **7**.

Temperature dependence of AC susceptibilities for **7** (Figure 8) clearly shows that the AC susceptibilities strongly depend on the frequency in both in- and out-of-phase. At 1.8 K, a Cole−Cole diagram (Supporting Information, Figure S16) from 1 to 1500 Hz in H_{dc} = 0 (χ_M'' vs χ_M') and the least-squares fitting by a Debye model gave a very small α value of 0.06, also indicating the distribution of a single relaxation process in **7**.

(16) (a) Aubin, S. M. J.; Sun, Z.; Pardi, L.; Krzystek, J.; Folting, K.; Brunel, L.-C.; Rheingold, A. L.; Christou, G.; Hendrickson, D. N. *Inorg. Chem.* **1999**, *38*, 5329. (b) Cole, K. S.; Cole, R. H. *J. Chem. Phys.* **1941**, *9*, 341.
(17) Kahn, M. L.; Mathonière, C.; Kahn, O. *Inorg. Chem.* **1999**, *38*, 3692.

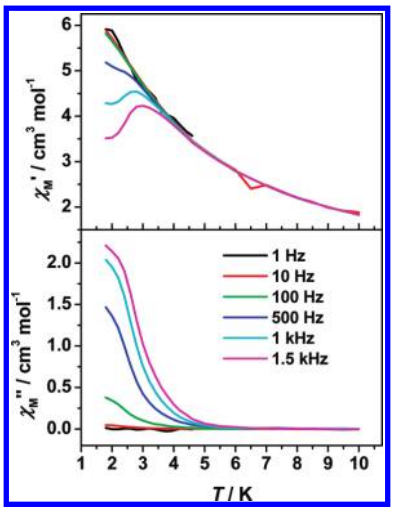

Figure 8. Temperature dependence of AC susceptibilities of **7** in H_{ac} = 3 Oe and H_{dc} = 0.

Undoubtedly, this result indicates that the slow magnetic relaxation of Dy^{III}-based complexes is irrelevant to the structure and the coupling interaction between ions (ground state spin $S = 0$ for antiferromagnetic system of **7**). Namely, the properties of single Dy^{III} ion may be directly responsible for the magnetic relaxation process of Dy^{III}-based complexes ($U = |D|J_{Dy}^2$). For confirming this conclusion, the investigations of magnetic properties for mononuclear Dy^{III} complexes are also under the way.

Complex **8** is an isolated mononuclear complex containing a Dy^{III} ion, in which there is not any strong interaction between molecules except van der Waals forces in the single crystal structure (Figure 3). Variable-temperature magnetic data of **8** were recorded in 100 Oe as shown in Figure 5d. Upon cooling from 300 to 1.8 K, $\chi_M T$ monotonicallly decreases from 14.20 to 10.83 cm^3 K mol^{-1} because of the thermal depopulation of Stark levels of the Dy^{III} ions. $\chi_M T$ at 1.8 K almost equals the literature value[17] of 21/2 cm^3 K mol^{-1} but much higher than that of **7** relative to one Dy^{III} ion because of no magnetic interaction between Dy^{III} ions. Therefore, the magnetic properties of **8** are the single-ion behavior of Dy^{III} ions.

AC measurements in a static field $H_{dc} = 0$ show that both in- and out-of-phase susceptibilities are strongly frequency dependent as expected (Figure 9 and Supporting Information, Figure S17), but without a clear peak. By virtue of the field of 2 kOe, a set of AC data with much better shape in χ_M'-T and χ_M''-T was obtained. Analyzing the slow dynamics of magnetization as a Cole−Cole diagram fitted by a Debye model (Figure 10), we found $\alpha = 0.07$, 0.07, and 0.04 at 1.8, 3, and 7 K with $H_{dc} = 0$, respectively.[16] When H_{dc} = 2 kOe, the α values are 0.18 and 0.13 at 3 and 7 K, respectively. These results indicate a single relaxation process in **8**. The relaxation time and the energy barrier can be estimated by the Arrhénius law to be $\tau_0 = 9.9 \times 10^{-7}$ s and 41 K, respectively (Supporting Information, Figure S18), which is close to that of **5**.

According to the magnetic results of **7** and **8**, it is surprising to find that the slow magnetic relaxation of Dy^{III}-containing complexes is independent of the interaction between Dy^{III} ions, or rather it is the intrinsic characteristic of a single ion. Factually, in lanthanide

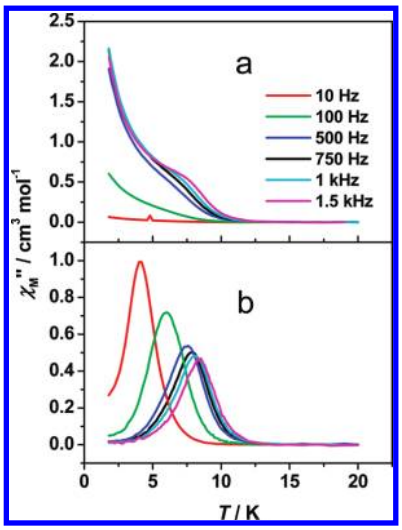

Figure 9. Temperature dependences of out-of-phase AC susceptibilities of **8** in H_{dc} = 0 (a) and 2 kOe (b) with H_{ac} = 3 Oe, respectively.

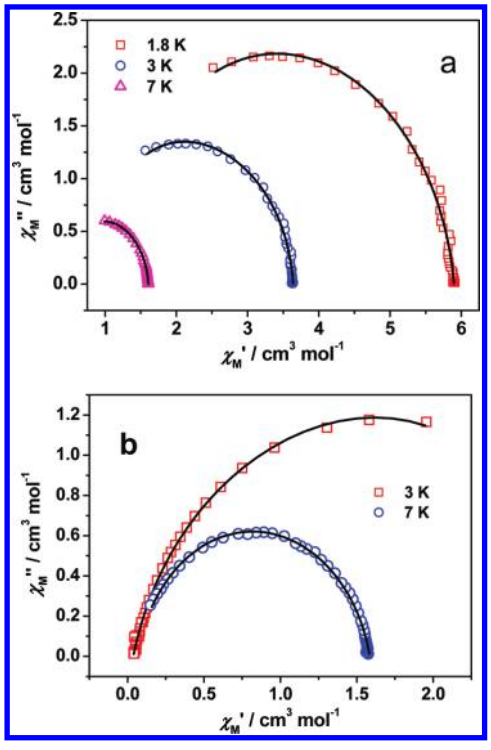

Figure 10. Cole−Cole diagram for **8** in H_{dc} = 0 (a) and H_{dc} = 2 kOe (b), respectively. The solid line represents the fitting with a Debye model.

complexes, the spin−spin superexchange interaction between Ln^{III} ions has not provided the main contribution to the magnetic properties any longer, because the 4f electrons of Ln^{III} ions are well-shielded by the outer s and p electrons. The superexchange coupling constant is usually lower by 2 orders of magnitude than the energy splittings resulting from LF effect. The long-range magnetic ordering in some Ln^{III} complexes is usually attributed to dipole−dipole interaction.[13a] The fitting results in **3** indicate that the spin−spin interaction between Ln^{III} ions is almost negligible in **1**−**6**. So, the magnetic properties of **5** mainly originate from the LF effect. It is well-known that a high-nuclear cluster shows the slow relaxation of magnetization, called SMM, if it possesses a high-spin ground state and a significantly large axial anisotropy. The L an^{III} ions such as Tb^{III}, Dy^{III}, Ho^{III}, and Er^{III} also have high spins and uniaxial anisotropy in complexes, and further lead to an energy barrier for spin reversal ($U = |D|J_z^2$) and $T_B \propto U$ (T_B is blocking temperature). So it is easy to be comprehended that they can display low-dimensional magnet behavior and slow magnetic relaxation process just like SMMs. To date, two typical structures of mononuclear Ln^{III} complexes have been reported by Ishikawa et al.[5a,c−e] and AlDamen et al.[5f] showing this kind of process. The theoretical studies indicates the Orbach process dominates the magnetic relaxation process in the mononuclear $[Pc_2Dy]^-$ complex.[18] For conveniently investigating the AC magnetic properties, a static field was applied in our experiments. The analytic results gave the energy barriers of **5**, **7**, and **8** close to 40 cm^{-1} calculated by Ishikawa et al.,[18] suggesting that they undergo the same relaxation process, although their ligands are different.

Conclusion

Applying furoic acid as a bridging ligand, a series of lanthanide complexes were isolated. X-ray single crystal diffraction analyses show that neighboring Ln^{III} ions in **1**−**6** were bridged by 2-furoate anions in *syn-anti* conformation to form a 1D alternative chain. This kind of carboxyl bridging mode leads to the antiferromagnetic interaction between light rare earth ions exemplified by Nd^{3+}, Sm^{3+}, and Gd^{3+} and ferromagnetic interaction between heavy rare earth ions such as Tb^{3+}, Dy^{3+}, and Er^{3+}. Interestingly, the frequency dependence of the AC magnetization was observed above 1.8 K in a Dy^{III}-based chain. Further magnetic investigations show the distribution of a single relaxation process in **5**. When the magnetic exploration was extended to other Dy^{III}-based complexes, the slow magnetic relaxation was also observed, especially in the antiferromagnetic coupling system of **7** with the ground state spin S = 0 or a mononuclear motif of **8**. Therefore, the slow magnetic relaxation of three Dy^{III}-containing complexes in this work results from the single-ion behavior of the Dy^{III} ion rather than from the spin−spin coupling interaction between the Dy^{III} ions.

Acknowledgment. This research was funded by the Major State Basic Research Development Program (2007CB925102 and 2006CB806104), National Natural Science Foundation of China (20721002, 20631030, and 20771057), and Postdoctoral Science Foundation of JiangSu Province (070219C).

Supporting Information Available: X-ray crystallographic data for complexes **1**−**8** in CIF format, Tables S1 and S2, and Figures S1−S4, and additionally magnetic analysis in Figures S5−S18. This material is available free of charge via the Internet at http://pubs.acs.org.

(18) Ishikawa, N.; Sugita, M.; Ishikawa, T.; Koshihara, S.; Kaizu, Y. *J. Phys. Chem. B* **2004**, *108*, 11265.